J|A|C|S
ARTICLES
Published on Web 02/22/2007

Calorimetric, Spectroscopic, and Model Studies Provide Insight into the Transport of Ti(IV) by Human Serum Transferrin

Arthur D. Tinoco, Christopher D. Incarvito, and Ann M. Valentine*

Contribution from the Department of Chemistry, Yale University, P.O. Box 208107, New Haven, Connecticut 06520-8107

Received November 14, 2006; E-mail: ann.valentine@yale.edu

Abstract: Evidence suggests that transferrin can bind Ti(IV) in an unhydrolyzed form (without bound hydroxide or oxide) or in a hydrolyzed form. Ti(IV) coordination by *N*,*N*′-di(*o*-hydroxybenzyl)ethylenediamine-*N*,*N*′-diacetic acid (HBED) at different pH values models the two forms of Ti(IV)-loaded transferrin spectrally and structurally. ^{13}C NMR and stopped-flow kinetic experiments reveal that when the metal is delivered to the protein using an unhydrolyzed source, Ti(IV) can coordinate in the typical distorted octahedral environment with a bound synergistic anion. The crystal structure of TiHBED obtained at low pH models this type of coordination. The solution structure of the complex compares favorably with the solid state from pH 3.0 to 4.0, and the complex can be reduced with $E_{1/2} = -641$ mV vs NHE. Kinetic and thermodynamic competition studies at pH 3.0 reveal that Ti(citrate)$_3$ reacts with HBED via a dissociative mechanism and that the stability of TiHBED ($\log \beta = 34.024$) is weaker than that of the Fe(III) complex. pH stability studies show that Ti(IV) hydrolyzes ligand waters at higher pH but still remains bound to HBED until pH 9.5. Similarly, at a pH greater than 8.0 the synergistic anion that binds Ti(IV) in transferrin is readily displaced by irreversible metal hydrolysis although the metal remains bound to the protein until pH 9.5. Thermal denaturation studies conducted optically and by differential scanning calorimetry reveal that Ti(IV)-bound transferrin experiences only minimal enhanced thermal stability unlike when Fe(III) is bound. The C- and N-lobe transition T_m values shift to a few degrees higher. The stability, competition, and redox studies performed provide insight into the possible mechanism of Ti_2−Tf transport in cells.

Introduction

Titanium(IV) compounds were investigated as a promising alternative to platinum antitumor agents because several were effective with lower side toxicity[1−6] and little cross-resistance with cisplatin.[7,8] Titanocene dichloride (Cp_2TiCl_2) and budotitane (Ti(bzac)$_2$(OEt)$_2$; Hbzac = 1-phenylbutane-1,3-dionato) entered clinical trials. Due to formulation problems budotitane did not pass phase I trials.[9−11] Titanocene dichloride advanced to phase II clinical trials in patients with metastatic renal-cell carcinoma and metastatic breast cancer, but the activity was found to be minimal.[12,13] The main problem with these compounds is the hydrolytic instability of Ti(IV), which results in precipitation of inactive titanium oxide species.[14,15]

While efforts are being made to synthesize Ti(IV) compounds with improved stability and increased cytotoxicity, little is still known about the antineoplastic mechanism of Ti(IV) drugs. Ti(IV) can inhibit intracellular enzymes[16] and bind to DNA,[17−20] but the details of the delivery route are unclear. A reasonable theory, proposed by Sadler et al., implicates serum transferrin in this mechanism.[21−23] Transferrin is an 80 kDa bilobal

(1) Christodoulou, C. V.; Ferry, D. R.; Fyfe, D. W.; Young, A.; Doran, J.; Sheehan, T. M. T.; Eliopoulos, A.; Hale, K.; Baumgart, J.; Sass, G.; Kerr, D. J. *J. Clin. Oncol.* **1998**, *16*, 2761−2769.
(2) Korfel, A.; Scheulen, M. E.; Schmoll, H. J.; Grundel, O.; Harstrick, A.; Knoche, M.; Fels, L. M.; Skorzec, M.; Bach, F.; Baumgart, J.; Sass, G.; Seeber, S.; Thiel, E.; Berdel, W. E. *Clin. Cancer Res.* **1998**, *4*, 2701−2708.
(3) Köpf, H.; Köpf-Maier, P. *Angew. Chem., Int. Ed. Engl.* **1979**, *18*, 477−478.
(4) Guo, Z. J.; Sadler, P. J. Medicinal inorganic chemistry. *Advances in Inorganic Chemistry*; 2000; Vol. 49, pp 183−306.
(5) Harding, M. M.; Mokdsi, G. *Curr. Med. Chem.* **2000**, *7*, 1289−1303.
(6) Caruso, F.; Rossi, M. Antitumor titanium compounds and related metallocenes. In *Metal Complexes In Tumor Diagnosis And As Anticancer Agents*; Sigel, A., Sigel, H., Eds; Metal Ions In Biolgical Systems; Marcel Dekker: New York, 2004; Vol. 42, pp 353−384.
(7) Harstrick, A.; Schmoll, H. J.; Sass, G.; Poliwoda, H.; Rustum, Y. *Eur. J. Cancer A* **1993**, *29A*, 1000−1002.
(8) Kurbacher, C. M.; Mallmann, P.; Kurbacher, J. A.; Sass, G.; Andreotti, P. E.; Rahmun, A.; Hubner, H.; Krebs, D. *Anticancer Res.* **1994**, *14*, 1961−1965.
(9) Clarke, M. J.; Zhu, F. C.; Frasca, D. R. *Chem. Rev.* **1999**, *99*, 2511−2533.
(10) Schilling, T.; Keppler, K. B.; Heim, M. E.; Niebch, G.; Dietzfelbinger, H.; Rastetter, J.; Hanauske, A. R. *Invest. New Drugs* **1995**, *13*, 327−332.
(11) Dubler, E.; Buschmann, R.; Schmalle, H. W. *J. Inorg. Biochem.* **2003**, *95*, 97−104.
(12) Lümmen, G.; Sperling, H.; Luboldt, H.; Otto, T.; Rubben, H. *Cancer Chemother. Pharmacol.* **1998**, *42*, 415−417.
(13) Kroger, N.; Kleeberg, U. R.; Mross, K.; Edler, L.; Sass, G.; Hossfeld, D. K. *Onkologie* **2000**, *23*, 60−62.
(14) Köpf-Maier, P.; Hesse, B.; Voigtländer, R.; Köpf, H. *J. Cancer Res. Clin. Oncol.* **1980**, *97*, 31−39.
(15) Ravera, M.; Cassino, C.; Monti, E.; Gariboldi, M.; Osella, D. *J. Inorg. Biochem.* **2005**, *99*, 2264−2269.
(16) Mokdsi, G.; Harding, M. M. *J. Inorg. Biochem.* **2001**, *83*, 205−209.
(17) Köpf-Maier, P.; Köpf, H. *Struct. Bonding* **1988**, *70*, 105−185.
(18) Köpf-Maier, P. *J. Struct. Biol.* **1990**, *105*, 35−45.
(19) McLaughlin, M. L.; Cronan, J. M.; Schaller, T. R.; Snelling, R. D. *J. Am. Chem. Soc.* **1990**, *112*, 8949−8952.
(20) Véra, J. L.; Román, F. R.; Meléndez, E. *Anal. Bioanal. Chem.* **2004**, *379*, 399−403.
(21) Sun, H. Z.; Li, H. Y.; Weir, R. A.; Sadler, P. J. *Angew. Chem., Int. Ed.* **1998**, *37*, 1577−1579.

10.1021/ja068149j CCC: $37.00

glycoprotein present in plasma at a concentration of about 35 μM.[24,25] It has a specific Fe(III) binding site located in each of the C- and N-lobes. Transferrin binds Ti(IV) from the active Ti(IV) drugs.[22] Ti(IV)-loaded transferrin is taken up by tumor cells, which also prevents binding of Fe(III)-loaded transferrin. In this mechanism, the starting Ti(IV) compounds serve only to deliver Ti(IV) to transferrin.[22] This scenario would explain why the structurally different titanocene dichloride and budotitane exhibit comparable activities. The determination that Ti(IV) binds to transferrin with greater affinity than Fe(III) supported this theory.[26] Tumor cells are known to have a significantly elevated iron requirement and expression of transferrin receptors than those of normal cells.[27−31] With Ti(IV) capable of competing with Fe(III) for transferrin binding and with transferrin receptors having a strong affinity for Ti(IV)-loaded transferrin,[22] tumor cells are naturally targeted for Ti(IV) uptake.

Transferrin may be the key to several features of the biochemistry of Ti(IV). The inherent solubility of Ti(IV) in water near neutral pH is quite low.[32,33] The K_{sp} (1×10^{-29}) is formulated for $TiO(OH)_2$.[32] At pH 7.4, this K_{sp} predicts a concentration of soluble titanium of 0.2 fM. The normal titanium concentrations in human blood serum (1−2 μM)[34,35] and milk (5.2 μM)[35] are much higher than the inherent solubility suggests. Still higher titanium concentrations can occur by several means. Certainly, direct injection with titanium compounds for imaging[36−38] or medicinal purposes[39] would result in elevated concentrations. Corrosion of Ti-containing implants affords a second mechanism.[40−44] Serum exposed to commercially pure Ti or a commonly used alloy can have up to 73 μM Ti.[42] Ingestion of TiO_2, a common pigment and filler, provides a final mechanism.[45] Proteins contribute to the elevated solubility of Ti in serum and other body fluids by binding the metal. Lactoferrin[46] may bind some of the Ti present in milk. Serum Tf is the principal protein that binds the highest concentration of Ti released in blood and may participate in transport of the metal.[37,38,47]

Chart 1

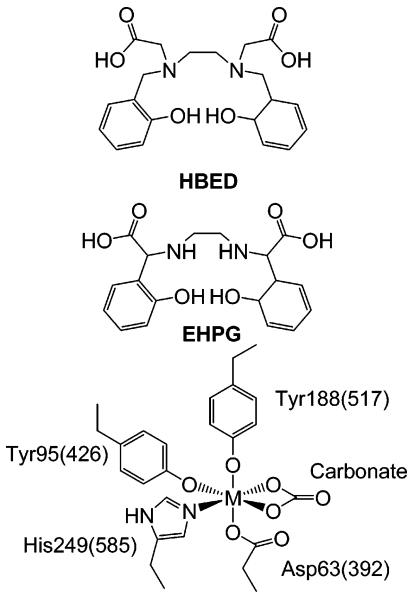

Transferrin binding site (C-lobe in brackets); idealized geometry

Further characterization of the interaction of Ti(IV) with transferrin may provide a better understanding of the transport of titanium into cells, and some insight is afforded by the study of model ligands. There is uncertainty as to how the metal ion is coordinated within the protein and how it could be released by the protein to the ultimate targets in the cell. Work with ligands that model the transferrin metal binding sites, which consist of two tyrosinates, one histidine, and one aspartate protein ligand, and a synergistic anion usually in the form of carbonate,[24] have helped shed light on these matters. The isomers of *N*,*N*′-ethylenebis(*o*-hydroxyphenylglycine) (EHPG) and *N*,*N*′-di(*o*-hydroxybenzyl)ethylenediamine-*N*,*N*′-diacetic acid (HBED) are appropriate model ligands in that they serve as hexadentate ligands capable of binding through the phenolate oxygens, the amine nitrogens, and the carboxylate oxygens (Chart 1). Monomer and dimer Ti(IV) complexes of EHPG isomers were synthesized,[48] which are seven coordinate unlike transferrin, with its distorted octahedral geometry. Recent work[49] on the bacterial ferric binding protein led to the suggestion that titanium may have been bound as a titanyl unit (TiO^{2+}) in the original studies of Ti(IV) interaction with transferrin.[21,22] Binding of metal oxo units by transferrin, for instance, a vanadium oxo species,[50] has been observed before, but titanyl binding may not be the only mode of Ti(IV) coordination.

(22) Guo, M. L.; Sun, H. Z.; McArdle, H. J.; Gambling, L.; Sadler, P. J. *Biochemistry* **2000**, *39*, 10023−10033.
(23) Messori, L.; Orioli, P.; Banholzer, V.; Pais, I.; Zatta, P. *FEBS Lett.* **1999**, *442*, 157−161.
(24) Lindley, P. F., Transferrins. In *Handbook of Metalloproteins*; Bertini, I., Ed.; Marcel Dekker: New York, 2001; Vol. 1, pp 793−811.
(25) Wally, J.; Halbrooks, P. J.; Vonrhein, C.; Rould, M. A.; Everse, S. J.; Mason, A. B.; Buchanan, S. K. *J. Biol. Chem.* **2006**, *281*, 24934−24944.
(26) Tinoco, A. D.; Valentine, A. M. *J. Am. Chem. Soc.* **2005**, *127*, 11218−11219.
(27) Faulk, W. P.; Hsi, B. L.; Stevens, P. J. *Lancet* **1980**, *2*, 390−392.
(28) Yeh, C. J. G.; Taylor, C. G.; Faulk, W. P. *Vox Sang.* **1984**, *46*.
(29) Panaccio, M.; Zalcberg, J. R.; Thompson, C. H.; Leyden, M. J.; Sullivan, J. R.; Lichtenstein, M.; McKenzie, I. F. C. *Immunol. Cell Biol.* **1987**, *65*, 461−472.
(30) Seymour, G. J.; Walsh, M. D.; Lavin, M. F.; Strutton, G.; Gardiner, R. A. *Urol. Res.* **1987**, *15*, 341−344.
(31) Cazzola, M.; Bergamaschi, G.; Dezza, L.; Arosio, P. *Blood* **1990**, *75*, 1903−1919.
(32) Babko, A. K.; Gridchina, G. I.; Nabivanets, B. I. *Russ. J. Inorg. Chem.* **1962**, *7*, 66−70.
(33) Einaga, H.; Komatsu, Y. *J. Inorg. Nucl. Chem.* **1981**, *43*, 2443−2448.
(34) Emsley, J. *The Elements*, 3rd ed.; Clarendon Press: Oxford, 1998.
(35) Lavi, N.; Alfassi, Z. B. *Analyst* **1990**, *115*, 817−822.
(36) Ishiwata, K.; Ido, T.; Monma, M.; Murakami, M.; Fukuda, H.; Kameyama, M.; Yamada, K.; Endo, S.; Yoshioka, S.; Sato, T.; Matsuzawa, T. *Appl. Radiat. Isot.* **1991**, *42*, 707−712.
(37) Vavere, A. L.; Laforest, R.; Welch, M. J. *Nucl. Med. Biol.* **2005**, *32*, 117−122.
(38) Vavere, A. L.; Welch, M. J. *J. Nucl. Med.* **2005**, *46*, 683−690.
(39) Melendez, E. *C. R. Oncol. Hematol.* **2002**, *42*, 309−315.
(40) Liu, T. K.; Liu, S. H.; Chang, C. H.; Yang, R. S. *Tohoku J. Exp. Med.* **1998**, *185*, 253−262.
(41) Kasai, Y.; Iida, R.; Uchida, A. *Spine* **2003**, *28*, 1320−1326.
(42) Hallab, N. J.; Skipor, A.; Jacobs, J. J. *J. Biomed. Mater. Res. A* **2003**, *65A*, 311−318.
(43) Strietzel, R.; Hosch, A.; Kalbfleisch, H.; Buch, D. *Biomaterials* **1998**, *19*, 1495−1499.
(44) Silwood, C. J. L.; Grootveld, M. *Biochem. Biophys. Res. Commun.* **2005**, *330*, 784−790.
(45) Bockmann, J.; Lahl, H.; Eckhert, T.; Unterhalt, B. *Pharmazie* **2000**, *55*, 140−143.
(46) Moshtaghie, A. A.; Ani, M.; Arabi, M. H. *Iran. Biomed. J.* **2006**, *10*, 93−98.
(47) Hallab, N. J.; Jacobs, J. J.; Skipor, A.; Black, J.; Mikecz, K.; Galante, J. O. *J. Biomed. Mater. Res.* **2000**, *49*, 353−361.
(48) Guo, M. L.; Sun, H. Z.; Bihari, S.; Parkinson, J. A.; Gould, R. O.; Parsons, S.; Sadler, P. J. *Inorg. Chem.* **2000**, *39*, 206−215.
(49) Guo, M. L.; Harvey, I.; Campopiano, D. J.; Sadler, P. J. *Angew. Chem., Int. Ed.* **2006**, *45*, 2758−2761.
(50) Chasteen, N. D.; Grady, J. K.; Holloway, C. E. *Inorg. Chem.* **1986**, *25*, 2754−2760.

Our previous work on the affinity of transferrin for Ti(IV)[26] supported quantitatively the work of Sadler.[21,22] One perplexing difference among the studies concerned the determined value of the molar absorptivity at 321 nm. The molar absorptivity for this tyrosine to Ti(IV) ligand to metal charge-transfer transition was determined to be 4830 M^{-1} cm^{-1} in the original work,[22] whereas we measured a value of 20 760 M^{-1} cm^{-1}.[26] These values are reported for total protein concentration. In both cases two equivalents of Ti(IV) were bound. We made a specific effort to avoid metal-induced hydrolysis of bound waters, resulting in a hydroxide-bound metal reagent, by using a highly water soluble and stable form of Ti(citrate)$_3$. It is believed that in that work Ti(IV) was coordinated to the protein in the more typical octahedral geometry, with a synergistic anion (probably carbonate) bound. This difference in coordination most likely underlies the significantly greater molar absorptivity that we measured.

To mimic Ti(IV) coordination and chemistry in this type of binding environment, chelation with HBED was attempted. While HBED is capable of binding a variety of metals, hard metals in particular, $HBED^{4-}$ binds Fe(III) most strongly (log $\beta = 39.01$).[51−57] Due to the stability and redox inertness of $FeHBED^-$,[58] HBED has been considered for treatment of iron-overload diseases.[59−65] HBED is structurally more flexible than EHPG, and this feature was suggestive that a TiHBED complex could be synthesized in the desired octahedral geometry.

In this work, Ti(IV) interactions with transferrin and the model HBED were probed via calorimetric and spectroscopic techniques. We report what factors affect the stability of Ti(IV) when bound in these environments. We also examine the effect on protein integrity that Ti(IV) coordination imposes. Finally, we discuss significant differences between Ti(IV) and Fe(III) bound transferrin with an emphasis on the feasibility of Ti(IV) transport in cells following the Fe(III) route.

Materials and Methods

Materials. All aqueous solutions were prepared with Nanopure-quality water (18.2 MΩ cm resistivity; Barnstead model D11931 water purifier). Human serum apotransferrin was purchased from Sigma. The purity of the protein was checked by Coomassie-stained SDS-PAGE and by dynamic light scattering using a Protein Solutions DynaPro 99 instrument, which showed only a monomeric protein species. The iron content was checked by ferrozine (Acros) assays and by monitoring the ligand to metal charge-transfer absorbance at 456 nm. The protein was typically apo as provided. HBED was purchased from Strem Chemical Co. Titanocene dichloride was obtained from Aldrich and prepared fresh in 1/9 DMSO/water, 0.1 M NaCl solution. Ti(citrate)$_3^{2-}$ ($K_2[Ti(C_6H_6O_7)_3]$) was prepared following a literature procedure and used for all competition studies.[66] ^{13}C-enriched bicarbonate (99%) was purchased from Cambridge Isotope Laboratories. Spectra/Por dialysis tubing (MWCO 10 kDa) was used for equilibrium dialysis. Amicon Centriprep centrifugal filters (MWCO 10 kDa) were used to concentrate protein samples. A titanium atomic absorption sample (1 mg/mL) was obtained from Aldrich and used for 2,3-dihydroxynaphthalene-6-sulfonate (TCI America) assays. Detergent compatible (DC) assay reagents were used from a Bio-Rad protein assay kit (Bio-Rad, Hercules, CA). All other chemicals were of high purity and used as received.

pH Measurements. The pH values were determined by using a ThermoOrion Model 410 meter and an Orion 8102BNUWP electrode, calibrated with Fisher Scientific buffer solutions at pH 4, 7, and 10. The pH meter measurements for D_2O solutions are recorded as uncorrected pH* values. The pH values were adjusted with calibrated HCl or KOH (DCl or NaOD).

Instrumentation. UV−vis spectra were recorded on a Cary 50 spectrophotometer (Varian). FT−IR spectra were collected on a Nicolet 6700 spectrometer using KBr pellets. Electrospray mass spectra were collected on a Waters/Micromass ZQ spectrometer at a capillary voltage of 3 kV, cone voltage of 20 V, and extractor voltage of 3V.

Characterization of TiHBED. Synthesis of [Ti(HBED)]·DMF. Ti(citrate)$_3^{2-}$ (0.542 mmol) and HBED (0.542 mmol) were each separately dissolved in 10 mL of water, with gentle warming (50 °C) to aid dissolution. The solutions were cooled to room temperature before the Ti(citrate)$_3^{2-}$ solution was added dropwise to the HBED solution. A yellow precipitate formed immediately in a final solution with pH 2.5. It was filtered and washed with water. The neutral complex is sparingly soluble in water. Yield: 0.22 g (0.508 mmol; 94%). CHN elemental analysis was performed by Atlantic Microlabs (Norcross, GA). Found (calcd): C, 55.70 (55.56); H, 4.76 (4.67); N, 6.42 (6.48). UV−vis (H_2O) at pH 3.0: $\lambda_{max} = 370$ ($\epsilon = 9141$ M^{-1} cm^{-1}). FT−IR data (cm^{-1}): $\nu_{as}(CO_2)$ 1694, 1573; $\nu_s(CO_2)$ 1482, 1453; ν(Ti-O) 921, 906. Mass spectrum (positive ion mode) at pH 3.0: $K[TiHBED]^+$-($m/z = 471$). The TiHBED precipitate was recrystallized in DMF, which resulted in crystals suitable for X-ray crystallography. ^{1}H NMR (ppm) at pH 3.0 50:50 DMSO/water: 3.336 (m); 3.820 (d of d); 4.275 (d of d); 6.780 (d); 7.025 (t); 7.286 (m); 7.321 (m). ^{13}C NMR (ppm) at pH 3.0 50:50 DMSO/water: 59.89; 60.96; 61.14;115.05; 122.87; 125.15; 129.95; 130.67; 160.01; 173.10.

NMR Spectroscopy. ^{1}H and proton-decoupled ^{13}C NMR solution spectra of HBED and TiHBED were recorded on Bruker 500 MHz instruments for 1D and 2D (HMQC and HMBC) experiments. A temperature variation study of TiHBED was done in acetone to access lower temperatures.

X-ray Structure Determination. A pale yellow blade crystal of TiHBED·DMF, $C_{23}H_{27}N_3O_7Ti$, having approximate dimensions of $0.20 \times 0.10 \times 0.08$ mm^3 was mounted with epoxy cement on the tip of a fine glass fiber. All measurements were made on a Nonius KappaCCD diffractometer with graphite monochromated Mo Kα radiation. The data were collected at a temperature of 173(2) K to a maximum 2θ value of 56.62°. Seven omega scans consisting of 37, 37, 34, 29, 24, 29, and 7 data frames, respectively, were collected with a frame width of 2.0° and a detector-to-crystal distance, Dx, of 38.0 mm. Each frame was exposed twice (for the purpose of de-zingering) for a total of 80 s. The data frames were processed and scaled using

(51) Ma, R.; Motekaitis, R. J.; Martell, A. E. *Inorg. Chim. Acta* **1994**, *224*, 151−155.
(52) Dyson, R. M.; Lawrance, G. A.; Mache, H.; Maeder, M. *Polyhedron* **1999**, *18*, 3243−3251.
(53) Bai, H.; Liu, W.; Yang, B. *Chin. J. Inorg. Chem.* **2001**, *17*, 389−394.
(54) Yang, B. S.; Feng, J. Y.; Li, Y. Q.; Gao, F.; Zhao, Y. Q.; Wang, J. L. *J. Inorg. Biochem.* **2003**, *96*, 416−424.
(55) Wang, J. L.; Bi, H. P.; Yang, B. S. *Guangpuxue Yu Guangpu Fenxi* **2005**, *25*, 89−91.
(56) Li, Y.; Qiao, Q.; Yang, X.; Yang, B. *Chin. J. Chem.* **2005**, *23*, 1361−1366.
(57) Taliaferro, C. H.; Motekaitis, R. J.; Martell, A. E. *Inorg. Chem.* **1984**, *23*, 1188−1192.
(58) Samuni, A. M.; Afeworki, M.; Stein, W.; Yordanov, A. T.; DeGraff, W.; Krishna, M. C.; Mitchell, J. B.; Brechbiel, M. W. *Free Radical Biol. Med.* **2001**, *30*, 170−177.
(59) Yinnon, A. M.; Theanacho, E. N.; Grady, R. W.; Spira, D. T.; Hershko, C. *Blood* **1989**, *74*, 2166−2171.
(60) Kalivendi, S. V.; Kotamraju, S.; Cunningham, S.; Shang, T.; Hillard, C. J.; Kalyanaraman, B. *Biochem. J.* **2003**, *371*, 151−164.
(61) Brittenham, G. M. *Alcohol* **2003**, *30*, 151−158.
(62) Bergeron, R. J.; Weigand, J.; Brittenham, G. M. *Blood* **2002**, *99*, 3019−3026.
(63) Sergejew, T.; Forgiarini, P.; Schnebli, H.-P. *Brit. J. Haematol.* **2000**, *110*, 985−992.
(64) Faller, B.; Spanka, C.; Sergejew, T.; Tschinke, V. *J. Med. Chem.* **2000**, *43*, 1467−1475.
(65) Grady, R. W.; Salbe, A. D.; Hilgartner, M. W.; Giardina, P. J. *Adv. Exp. Med. Biol.* **1994**, *356*, 351−359.
(66) Zhou, Z. H.; Deng, Y. F.; Jiang, Y. Q.; Wan, H. L.; Ng, S. W. *Dalton Trans.* **2003**, *13*, 2636−2638.

the DENZO software package.[67] A total of 9758 reflections were collected of which 5778 were unique and observed ($R_{int} = 0.0435$). The linear absorption coefficient, μ, for Mo Kα radiation is 4.14 cm^{-1}, and no absorption correction was applied. The data were corrected for Lorentz and polarization effects. The structure was solved by direct methods and expanded using Fourier techniques.[68] The non-hydrogen atoms were refined anisotropically, and hydrogen atoms were treated as idealized contributions. Relevant crystallographic data are presented in Table S1.

pH Stability Study. A 50 mL solution of 259 μM TiHBED was prepared at pH 0.6 (3.2% DMSO aqueous solution). Aliquots of 0.1011 M KOH were added to monitor the stability of the complex up to pH 10 at 298 K while following the change of the UV−vis and ^{1}H NMR spectra.

Cyclic Voltammetry. Cyclic voltammograms were measured by using a Metrohm 746 VA Trace Analyzer and a 747 VA stand. A hanging drop mercury electrode was the working electrode, Ag/AgCl/3M KCl was the reference electrode, and a platinum wire was used as the auxiliary electrode. The potentials are reported vs NHE. All solutions were purged with nitrogen. The voltammograms of 4 mM solutions of HBED and TiHBED in 0.1 M KNO_3 solution (50:50 water/acetonitrile) at pH 4.0 and 8.36 were recorded at a scan rate of 25 mV s^{-1}.

Fluorescence Study. The fluorescence emissions ($\lambda_{ex} = 280$ nm) of 25 μM HBED and TiHBED prepared in DMF were monitored by using a Photon Technology International QM-4 spectrofluorometer. The excitation and emission slit widths were 1 nm.

Kinetics Study. A ligand substitution experiment was performed in water at pH 3.0 (25 °C, I = 0.1 M) under pseudo-first-order conditions. The [citrate] was varied from 1 to 10 mM, while the [Ti(IV)] and [HBED] were maintained at 50 μM and 0.56 mM, respectively. The [HBED] was varied from 0.5 to 5 mM, while the [Ti(IV)] and [citrate] were maintained at 25 μM and 2.5 mM, respectively. The kinetics experiments, performed in triplicate, were followed by monitoring the formation of the TiHBED LMCT band at 370 nm by UV−vis. A temperature variation (8 to 45 °C) experiment was performed monitoring the reaction of 25 μM Ti(IV) with 1.26 mM HBED and 2.5 mM citrate. The data were analyzed fitting exponentials by using Origin 6.0 and by using Dynafit (version 3.28.40).[69]

Equilibrium Binding Studies of TiHBED. A spectrophotometric ligand competition experiment was performed at pH 3.0 (25 °C, I = 0.1 M). Solutions of 1 mL of 26.45 μM Ti(citrate)$_3^{2-}$ in 7.00 mM citrate with varying concentrations of HBED (0 to 515 μM) were allowed to equilibrate for 2 days and then scanned by UV−vis (300 to 500 nm). A saturation curve of absorbance at 370 nm versus [HBED] was fitted with the following equation:[70]

$$A = [A_{max}(K[Ti]_o + K[HBED]_o + 1) - A_{max}(K[Ti]_o + K[HBED]_o + 1)^2 - 4K^2[Ti]_o[HBED]_o^{0.5}]/2K[Ti]_o \quad (1)$$

$[Ti]_o$ and $[HBED]_o$ are the initial concentrations and A_{max} is the maximum absorbance. The full spectra were also fitted by SpecFit/32.[71]

Characterization of Ti(IV)-Loaded Transferrin. Kinetics Studies. Unless mentioned otherwise, all transferrin reactions were performed in air-saturated solution, which contains 129 μM bicarbonate.[72] Apotransferrin (18.6 μM) was prepared in a 50 mM Tris, 10 mM Na_3-Citrate, 140 mM NaCl, I = 0.2 M, pH 7.4 buffer at 25 °C. Ti(citrate)$_3^{8-}$ solutions (0.402 mM) were prepared in the same buffer with varying bicarbonate concentrations (0.4 to 8.4 mM). The kinetics were monitored by following the growth of the tyrosine to Ti(IV) LMCT band at 321 nm. The experiment was performed on a Kintek stopped-flow 2001 instrument. Observed rate constants were calculated by fitting exponentials using Origin 6.0.

NMR Spectroscopy. Following extensive water dialysis and lyophilization, a 1 mM transferrin solution was prepared in 450 μL of 10 mM (pH* 7.4) Tris buffer (30:70 D_2O/H_2O, 10 mM $H^{13}CO_3^-$, 190 mM NaCl, I = 0.2 M). 2 mol equiv of 8 mM Ti(citrate)$_3^{8-}$ were added to the protein solution. The solution was allowed to equilibrate for 2 days. The solution was diluted to 15 mL and then rapid-spin concentrated to 450 μL to remove any unbound material. Approximately 25 000 scans were collected for a proton decoupled ^{13}C experiment on a Bruker 500 MHz instrument, and the spectrum was analyzed with a line broadening of 10 Hz.

Fluorescence Study. The change in the fluorescence emission ($\lambda_{ex} = 280$ nm) of transferrin due to Ti(IV) binding was monitored. Apotransferrin was extensively dialyzed in 0.1 M Tris pH 7.4, with 0.1 M NaCl, 10 mM $NaHCO_3$, and 1 mM citrate. Separate solutions (200 μL), which consisted of 25 μM transferrin and varying mole equivalents of Ti(citrate)$_3^{8-}$ (0.2 to 4.4), were prepared and equilibrated for 2 days at 25 °C. The excitation and emission slit widths were 1 nm.

pH Stability Studies. A 10 mL Ti(IV)-loaded transferrin (Ti_2Tf) sample (9.67 μM) was prepared with excess Ti(citrate)$_3^{8-}$ in pH 7.4 Tris buffer (0.1 M NaCl, 20 mM $NaHCO_3$, and 10 mM Na_3Citrate). The protein was extensively dialyzed in 0.1 M NaCl. The solution was evenly divided to titrate one-half to higher pH and the other half to lower pH. The pH was adjusted by slow addition of 0.1 M HCl or 0.1 M NaOH. Aliquots at each pH were scanned by UV−vis.

Thermal Protein Unfolding Measurements. The buffer for all unfolding experiments was 500 mM Hepes (pH 7.4) with 20 mM $NaHCO_3$. Differential scanning calorimetry (DSC) experiments were performed on a MicroCal VP Capillary instrument (MicroCal Inc., Northampton, MA) and used 25 μM transferrin in the presence of varying equivalents of Ti(IV) supplied by Ti(citrate)$_3^{8-}$ or titanocene dichloride. The solutions were allowed to equilibrate at 25 °C for 12 h. In the Ti(citrate)$_3^{8-}$ experiments 10 mM citrate was included. The scan rate was 81.5 °C/h. Origin 7.0 software was used for data analysis.

The reversibility of thermal unfolding of 11.7 μM Ti_2−Tf was examined optically by using a Cary 100 spectrophotometer (Varian). The temperature of the protein sample was raised from 20 to 95 °C and then lowered from 95 to 20 °C at a scan rate of 30 °C/h while following the 321 nm LMCT absorbance. Transition temperatures were determined from the derivative plots of absorbance versus temperature.

Ti(IV) Quantitation. The Ti(IV) content in transferrin samples was quantified spectrophotometrically by chelation with 2,3-dihydroxynaphthalene-6-sulfonate by using a standard addition method. To 500 μL of protein sample was added 500 μL of denaturing solution (5% trichloroacetic acid in 0.5 M HCl). The mixture was extensively boiled and then centrifuged to separate the protein precipitate. Solutions with internal standards (5 to 20 μM) were prepared to a total volume of 500 μL in a 1.81 M acetate buffer (pH 5.2). These solutions included 50 μL of the denatured protein solution and 250 μL of a 25 mM 2,3-dihydroxynaphthalene-6-sulfonate solution prepared in the same buffer. A blank solution was prepared that included no protein sample but instead 25 μL of denaturing solution and 25 μL of dialysis buffer. The solution absorbances at 370 nm (ϵ = 40 000 M^{-1} cm^{-1}) versus titanium concentration were plotted after correcting for the absorbance of the blank. Control experiments verified that Ti(IV) is bound at a specific high affinity site of the protein. The Ti(IV) content was measured from samples in which the protein had not been denatured. Nearly 1 day is required for solutions to reach equilibrium for the nondenatured protein samples versus about 0.5 hour for the denatured protein as measured

(67) Otwinowski, Z.; Minor, W. Processing of X-ray diffraction data collected in oscillation mode. In *Macromolecular Crystallography, Pt A*; Carter, C. W., Jr., Sweet, R. M., Eds.; Academic Press: San Diego, CA, 1997; Vol. 276, pp 307−326.
(68) Sheldrick, G. M. *Acta Crystallogr.* **1990**, *A46*, 467−473.
(69) Kuzmič, P. *Anal. Biochem.* **1996**, *237*, 260−273.
(70) Bertsch, M.; Mayburd, A. L.; Kassner, R. J. *Anal. Biochem.* **2003**, *313*, 187−195.
(71) Binstead, R. A.; Jung, B.; Zuberbuhler, A. D. *Specfit/32*; Software Associates: Marlborough, MA, 2001.
(72) Benjamin, M. M. *Water Chemistry*; McGraw Hill Inc.: Boston, 2002; p 668.

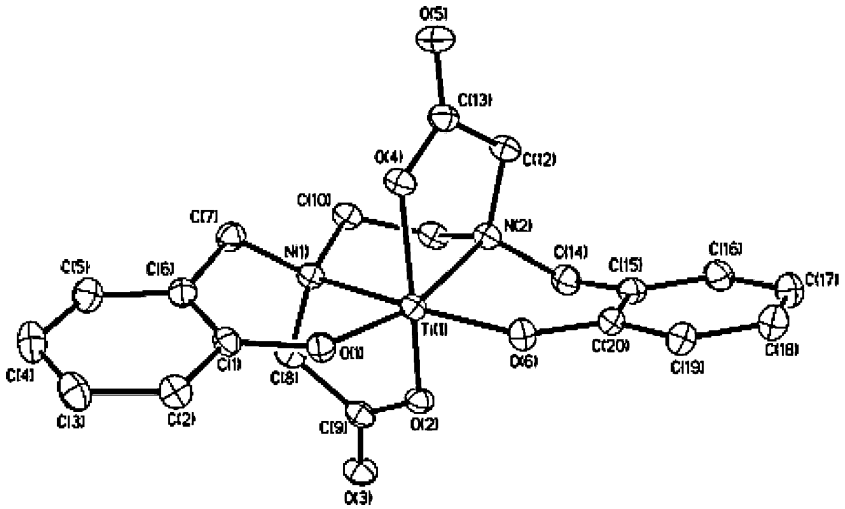

Figure 1. ORTEP diagram of TiHBED.

by repeated assays. The Ti(IV) content measured for the nondenatured protein is consistently lower than (typically a factor of 2 or more) that for the denatured protein implying that the Ti(IV) is bound to a high affinity site from which 2,3-dihydroxynaphthalene-6-sulfonate cannot fully remove it at this pH.

Results

Solid-State Characterization of TiHBED. TiHBED crystallized with DMF in the triclinic space group $P\bar{1}$ with one molecule in the asymmetric unit and two molecules in the unit cell. The ORTEP diagram for the complex is shown in Figure 1, and selected bond distances and angles are given in Table S2. The geometry about the titanium atom is pseudo-octahedral. The complex possesses a twofold rotation axis which bisects the O(1)−Ti(1)−O(6), N(1)−Ti(1)−N(2), and O(2)−Ti(1)−O(4) angles.

The FT−IR spectrum of TiHBED shows asymmetric carbonyl stretches at 1694 and 1573 cm^{-1} and symmetric stretches at 1482 and 1453 cm^{-1}. These stretches are shifted to lower frequency relative to the spectrum of HBED. The differences between the asymmetric and symmetric stretches are greater than 200 cm^{-1} and indicate carboxylate binding in monodentate form.[73]

Studies of TiHBED in Solution. The optical and ^{1}H NMR spectra of 259 μM TiHBED were monitored at different pH values. A small amount (3.2%) of DMSO was required for complex solubility. Below pH 1.5, minimal complex formation is observed as the optical spectrum is comparable to uncomplexed HBED (data not shown), which is also true of the aromatic protons of the ^{1}H NMR spectra (Figure S1). The LMCT band due to chelation by the phenolates is observed centered at 370 nm (ϵ = 9141 M^{-1} cm^{-1}) (Figure 2). The species is stable from pH 3.0 to 4.0. A new species develops above pH 6.0. The maximum signal for the LMCT band of this species is observed at pH 7.47 with λ_{max} = 306 nm (ϵ = 4570 M^{-1} cm^{-1}). The ^{1}H NMR spectra from pH 6.0 to pH 9.0 show a mixture of Ti(IV) species. Above pH 9.5 no LMCT band is observed and the ^{1}H NMR spectrum is similar to that of uncomplexed HBED (Figure S1). A white precipitate is observed above pH 10.

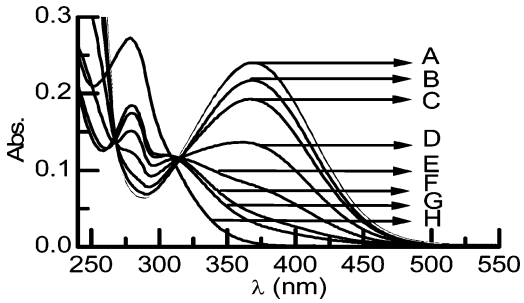

Figure 2. UV−vis spectra (path length 0.1 cm) of 259 μM TiHBED (3.2% DMSO) at various pH values. (A) pH 3.0−4.0; (B) pH 5.00; (C) pH 5.49; (D) pH 6.00; (E) pH 6.49; (F) pH 7.08; (G) pH 7.47; (H) pH 9.57.

The electrospray mass spectrum of 1 mM TiHBED at pH 3.0 supports the finding that the complex remains intact in solution (Figure S2). A single Ti(IV) signal is consistent with the titanium isotope distributions for $K[TiHBED]^+$ (m/z = 471). ^{1}H and ^{13}C NMR spectra (50:50 DMSO/water at pH 3.0) helped to characterize the solution structure of TiHBED (Figure S3 and S4). Identification of all proton and carbon peaks was done by using the 2D NMR techniques HMQC and HMBC.[74] The chemical shifts and assignments are shown in Table S3. Coordination to Ti(IV) shifts all of the proton and carbon resonances of HBED. The ethylenediamine protons are magnetically inequivalent because the ethylenediamine portion of HBED is oriented in a gauche conformation. A temperature variation experiment was undertaken in acetone to determine if any structural fluctuations occur in solution (Figure S5). The coupling pattern of the ethylenediamine protons appears to be solvent- and temperature-dependent. Solvation effects result in a singlet pattern at lower temperatures. At temperatures greater than 25 °C in acetone, the expected AA′BB′ pattern was observed.

The fluorescence emission of HBED alone could not be monitored in aqueous solution at pH 3.0 because the signal was unstable possibly due to ligand aggregation. A comparison of the fluorescence emission between HBED and TiHBED (25 μM of both) could be obtained in DMF at 25 °C (Figure S6). Binding of Ti(IV) quenched the HBED emission signal at 330 nm to 25% of the original signal.

(73) Deacon, G. B.; Phillips, R. J. *Coord. Chem. Rev.* **1980**, *33*, 227−250.

(74) Wilson, J. G. *Aust. J. Chem.* **1988**, *41*, 173−182.

The cyclic voltammogram of 4 mM HBED in the range of 0.293 to −1.5 V (vs NHE) showed no redox activity at either pH 4.0 or 8.36 (data not shown). At pH 4.0 the cyclic voltammogram of 4 mM TiHBED showed a nearly reversible redox couple with E_{red} at −673 mV and E_{ox} at −609 mV (Figure S7). The ΔE for the system is 64 mV, and the reduction potential ($E_{1/2}$) calculated is −641 mV (vs NHE). At pH 8.36 three signals were observed: a reversible redox couple with $E_{1/2} = -600$ mV and two irreversible peaks with E_{red} at −947 mV and E_{red} at −1162 mV (Figure S7).

The kinetics of TiHBED formation were investigated to explore how transferrin might complex Ti(IV). In these experiments, Ti(citrate)$_3$ was reacted with HBED and the ligand substitution was monitored by following the development of the LMCT band (370 nm) of TiHBED (Figure S8). The experiments were performed under pseudo-first-order conditions with citrate and HBED in excess. All data could be fit with a single exponential to calculate observed rate constants. Due to the complex speciation of the ligands at pH 3.00, all fits were made with total citrate and HBED concentrations without regard to protonation states, assuming fast equilibrium among species.[57,75] Figure 3 shows the dependence of the observed rate constant on total citrate and HBED concentration. The rate of TiHBED formation decreases with an increase in citrate concentration until it approaches zero at high concentrations. The rate of TiHBED formation increases linearly with an increase in HBED concentration. Based on these data and simulation with the software Dynafit, the following mechanism was proposed to describe TiHBED formation:

$$\mathrm{Ti(citrate)_3} \overset{K_1}{\rightleftharpoons} \mathrm{Ti(citrate)_}x + (3-x)\mathrm{Citrate}$$

$$\mathrm{Ti(citrate)_}x + \mathrm{HBED} \xrightarrow{k_2} \mathrm{TiHBED} + x\mathrm{Citrate}$$

The first step involves a rapid equilibrium in which the Ti(citrate)$_3$ complex dissociates releasing one to three of the citrates. The second step is a slower process involving the chelation of Ti(IV) by HBED, so that

$$k_{obsd} = \frac{k_2 K_1 [\mathrm{HBED}]}{[\mathrm{citrate}]^{3-x} + K_1} \qquad (2)$$

The kinetics data could best be fitted to eq 2 when invoking only one citrate released. Both Ti(citrate)$_2$ ($H[Ti(C_6H_5O_7)_2]^-$; $m/z = 427.33$) and Ti(citrate)$_3$ species ($K[Ti(C_6H_6O_7)_3]^-$; $m/z = 657.2$) could be detected by electrospray mass spectrometry in a 1 mM, pH 3.0 solution, which suggests that Ti(IV) coordination by citrate is very labile (Figure S9). The values of K_1 and k_2 were determined to be 2.65 ± 0.11 mM and 9.28 ± 0.18 M^{-1} s^{-1}, respectively.

A temperature variation experiment was also performed. Dynafit was used to calculate k_2 values. Figure S10 shows Arrhenius and Eyring plots of the temperature variation data.[76] The activation energy determined was 64.4 kJ mol^{-1}. The values of $\Delta H^{\ddagger}$ and $\Delta S^{\ddagger}$ were 61.7 kJ mol^{-1} and −20.3 J mol^{-1} K^{-1}, respectively.

(75) Collins, J. M.; Uppal, R.; Incarvito, C. D.; Valentine, A. M. *Inorg. Chem.* **2005**, *44*, 3431−3440.
(76) Jordan, R. B. *Reaction Mechanisms of Inorganic and Organometallic Systems*, 2nd ed.; Oxford University Press, Inc.: New York, 1998.

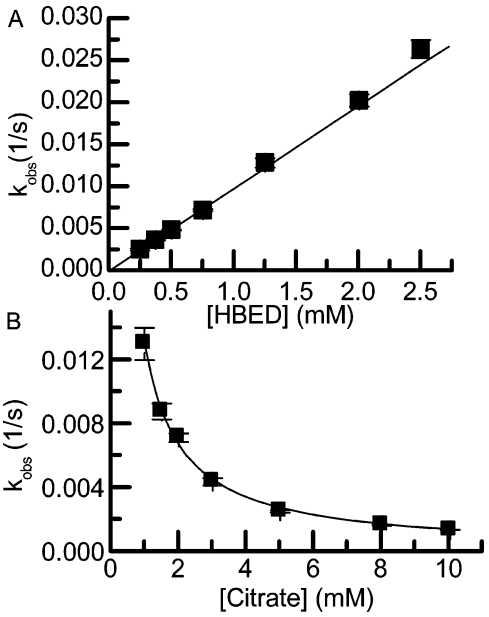

Figure 3. Dependence of the observed rate constant for TiHBED formation on (A) HBED and (B) citrate concentration with 50 μM Ti(citrate)$_3^{2-}$ and 2.5 mM citrate (varying HBED concentrations) and 560 μM HBED (varying citrate concentrations), respectively. Reaction conditions: pH 3.00, 25 °C, and $I = 0.1$ M. Each point is the average of at least three determinations, and the error bars, when not visible, are smaller than the data points.

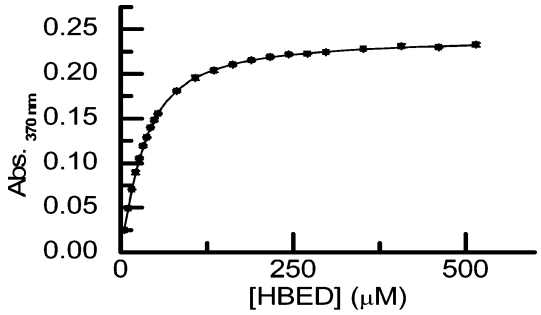

Figure 4. Absorbance at 370 nm versus [HBED] obtained from the reaction of 26.45 μM Ti(citrate) species with different concentrations of HBED in the presence of 7.00 mM citrate at pH 3.00. K_{app} was determined to be 48 400 ± 400.

Equilibrium binding studies of TiHBED were performed by competition with citrate at pH 3.00. The complex speciation of all reactants was considered to quantify the TiHBED affinity constant (Table S4).[57,75] An apparent binding constant (K_{app}) was determined from the reaction of 26.45 μM Ti(citrate) species in 7.00 mM citrate buffer with increasing concentrations of HBED (0 to 515 μM) (Figure 4).

K_{app} was determined to be 48 400(400) (log $K = 4.685$) by using eq 1. K_{app} was corrected for the overall equilibrium.

$$\begin{aligned} &0.0036\ \mathrm{Ti(C_6H_5O_7)^+} + 0.9849\ \mathrm{Ti(C_6H_6O_7)_3^{2-}} \\ &+ 0.0115\ \mathrm{Ti(C_6H_6O_7)(C_6H_5O_7)_2^{4-}} + 0.0154\ \mathrm{C_{20}H_{23}N_2O_6^-} \\ &+ 0.7391\ \mathrm{C_{20}H_{24}N_2O_6} + 0.2337\ \mathrm{C_{20}H_{25}N_2O_6^+} \\ &+ 0.0117\ \mathrm{C_{20}H_{26}N_2O_6^{2+}} \end{aligned} \overset{K}{\rightleftharpoons}$$

$$\begin{aligned} &\mathrm{Ti(C_{20}H_{20}N_2O_6)} + 0.0808\ \mathrm{C_6H_6O_7^{2-}} \\ &+ 1.6493\ \mathrm{C_6H_7O_{7-}} + 1.2627\ \mathrm{C_6H_8O_8} \\ &+ 0.0400\ \mathrm{H^+} \end{aligned}$$

$$K = K_{app}[\mathrm{C_6H_6O_7^{2-}}]^{0.0808}[\mathrm{C_6H_7O_7^-}]^{1.6493}[\mathrm{C_6H_8O_7}]^{1.2627}[\mathrm{H^+}]^{0.04} \qquad (3)$$

K was determined to be 1.649×10^{-4}.

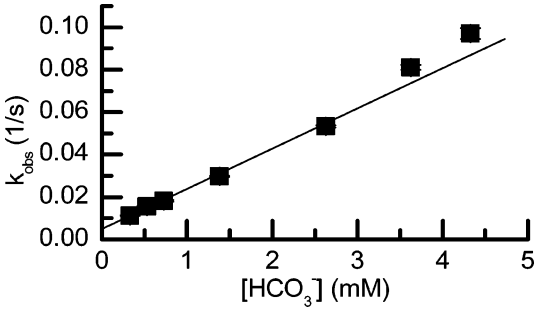

Figure 5. Plot of observed rate constant (k_{obsd}) of the initial phase of Ti_2−Tf formation versus [HCO_3^-]. The experiment was performed at pH 7.4 and 25 °C (50 mM Tris buffer, 0.1 M NaCl, 10 mM Na_3Citrate).

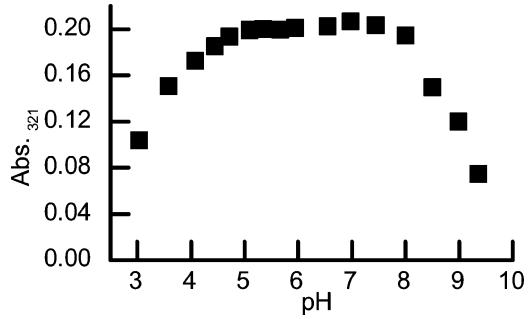

Figure 6. pH stability of 9.8 μM Ti_2−Tf in 0.1 M NaCl monitored following the change of the LMCT absorbance at 321 nm.

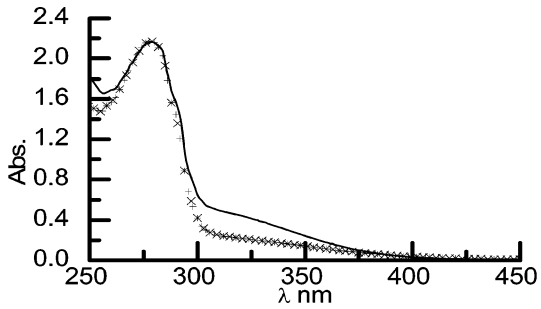

Figure 7. UV−vis spectrum of Ti_2−Tf following loading with Ti(citrate)$_3^{8-}$ in the presence of 10 mM Na_3Citrate and 20 mM $NaHCO_3$ at pH 7.4 (solid line) and the UV−vis spectra following dialysis at pH 8.5 in the presence (+) and absence (×) of 10 mM Na_3Citrate and 20 mM $NaHCO_3$.

SpecFit was also utilized to derive K_{app}. A simple model in which Ti(citrate) species were treated as a single metal species and HBED species were treated as a single ligand species accounted for all colored species well (Figure S11). The log K_{app} value (4.659 ± 0.005) compares favorably. Table S5 reports all of the individual equilibria and corresponding stability constants. By careful consideration of all equilibria, the TiHBED binding constant was determined to be log $\beta = 34.074 \pm 0.004$.

Ti(IV) Coordination by Human Serum Transferrin (Tf). Transferrin (9.3 μM) was reacted with Ti(citrate)$_3^{8-}$ (201 μM) in the presence of 10 mM citrate with varying concentrations of bicarbonate, and the initial phase of Ti_2−Tf formation was monitored. The dependence of the observed rate constant on bicarbonate concentration is linear (Figure 5). In the absence of bicarbonate, the observed rate constant is lower but the overall absorbance change is similar suggesting that citrate may serve as a synergistic anion.

The ^{13}C NMR spectrum in the carbonyl region of 1 mM Ti_2−Tf shows a signal at 166.1 ppm, which indicates coordinated bicarbonate (most likely in the form of bidentate carbonate) (Figure S12).[77] Because the source of Ti(IV) in this experiment was Ti(citrate)$_3^{8-}$ there had been the possibility that citrate would serve as a synergistic anion. It appears that, with high enough concentration, bicarbonate can displace citrate when Ti(IV) is coordinated by transferrin. The signal for bound carbonate remained for at least several weeks.

The fluorescence emission spectra of transferrin at 322 nm (λ_{ex} = 280 nm) in the presence of increasing equivalents of Ti(IV) show that two Ti(IV) ions bind but that at these concentrations the protein is not saturated until four equivalents are added (Figure S13). Ti(IV) saturation of transferrin quenched the protein emission by 73%.

pH Stability of Ti_2−Tf. The stability of the Ti_2−Tf complex was monitored at varying pH values. Aliquots (500 μL) from a stock protein solution that had been carefully equilibrated to a particular pH were removed and scanned by UV−vis. Maximum absorbance of the Ti_2−Tf LMCT band (λ_{max} = 321 nm) was maintained from pH 5 to 7.5 (Figure 6). The aliquots of the protein solution at pH 3.0, 8.5, and 9.5 were extensively dialyzed in 0.1 M NaCl. No change in protein concentration was observed as indicated by the absorbance at 280 nm. After dialysis 1 equiv of Ti(IV) remained in the pH 3.0 sample, whereas no Ti(IV) remained in the pH 9.5 sample. 2 equiv of Ti(IV) still remained in the pH 8.5 sample. Another Ti_2−Tf sample was prepared and immediately dialyzed at pH 8.5 in the presence and absence of 20 mM bicarbonate and 10 mM citrate. The LMCT absorbance decreases following dialysis in either experiment, but the Ti(IV) content does not change (Figure 7). The molar absorptivity at 321 nm decreases from 20 780 M^{-1} cm^{-1} to 9780 M^{-1} cm^{-1}. The latter value is comparable to that reported for Ti(IV) bound to transferrin in the absence of bicarbonate,[22] which suggests that the bound synergistic anion is labile at pH 8.5. The synergistic anion is most likely displaced by hydroxides.

Thermal Stability of Ti_2−Tf. Differential scanning calorimetric experiments were conducted to probe the change in transferrin stability due to Ti(IV) binding. Ti(IV) was delivered to the protein as the triscitrate complex, which we believe not to include coordinated hydroxide at pH 7.4.[75] Ti(IV) was also delivered as titanocene dichloride, which will react to produce bound hydroxides at this pH.[78] The apparent molar absorptivities at 321 nm of the two forms compared favorably with published values.[22,26] The protein was scanned in the presence of different mole equivalents of Ti(IV) (Figure 8). All transitions were fitted to a two-state model (Table 1). The addition of 1 equiv of Ti(IV) in both experiments results in three transitions, one of which corresponds to the N-lobe (higher T_m) and the other two which correspond to the C-lobe.[79] The unfolding of the Ti_2−Tf complex is not thermodynamically but instead kinetically controlled, which is also true of the Fe_2−Tf complex,[79] as confirmed by the thermal denaturation of 11.7 μM Ti_2−Tf monitored optically (Figure S14). Ti(IV) does not rebind to thermally denatured transferrin when the temperature is lowered to room temperature.

(77) Bertini, I.; Luchinat, C.; Messori, L.; Scozzafava, A.; Pellacani, G. *Inorg. Chem.* **1986**, *25*, 1782−1786.
(78) Toney, J. H.; Marks, T. J. *J. Am. Chem. Soc.* **1985**, *107*, 947−953.
(79) Lin, L. N.; Mason, A. B.; Woodworth, R. C.; Brandts, J. F. *Biochemistry* **1994**, *33*, 1881−1888.

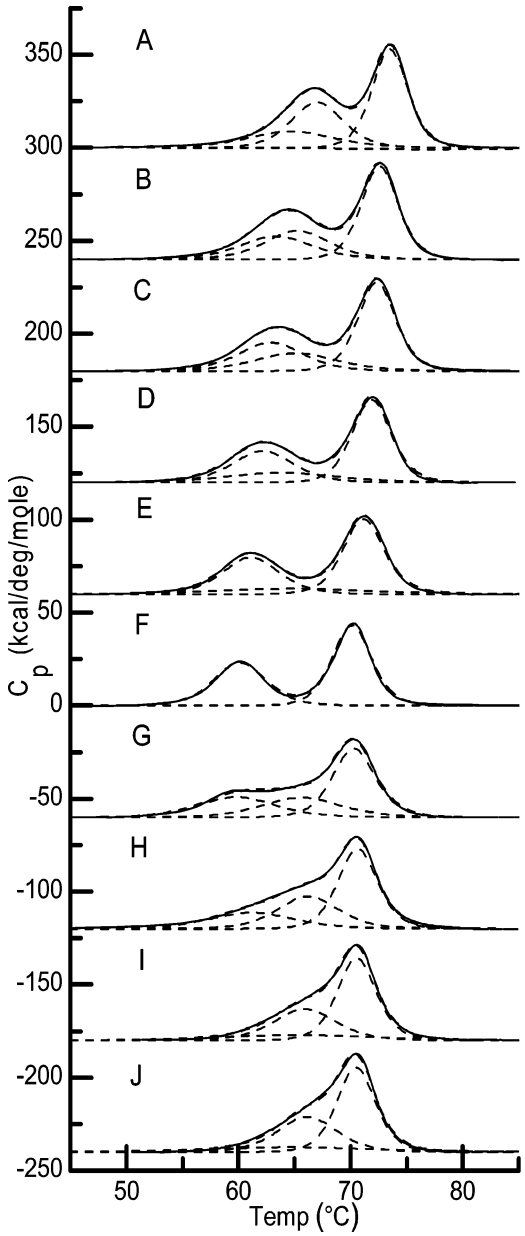

Figure 8. DSC thermograms (baseline corrected) of 25 μM human serum transferrin in the absence (F) or presence of $Ti(citrate)_3^{8-}$ (A−E) and titanocene dichloride (G−J) at various molar ratios in 500 mM Hepes, 25 mM $NaHCO_3$, pH 7.4. $Ti(citrate)_3^{8-}$ experiment: (A) 10 equiv of Ti; (B) 2 equiv of Ti; (C) 1.5 equiv of Ti; (D) 1 equiv of Ti; (E) 0.5 equiv of Ti. Titanocene dichloride experiment: (G) 0.5 equiv of Ti; (H) 1 equiv of Ti; (I) 1.5 equiv of Ti; (J) 2 equiv of Ti.

Discussion

Characterization of TiHBED. Ti(IV) coordination by $HBED^{4-}$ is different from its coordination by $EHPG^{4-}$. $HBED^{4-}$ complexes Ti(IV) similar to the Fe(III) coordination in $FeHBED^-$,[80] in a pseudo-octahedral geometry with the carboxylate oxygens trans to each other and the phenolate oxygens cis to each other. The seven coordinate TiEHPG structure, on the contrary, is surprising considering that $FeEHPG^-$ is six-coordinate and the phenolate oxygens of both isomers coordinate cis to each other.[81] The position of the carboxylates on the α-benzyl carbon of EHPG may cause steric restraints upon Ti(IV) coordination. The structure of TiHBED is thus more similar to the typical mode of metal binding in transferrin, in which the tyrosinate oxygens are coordinated cis to one another.

Table 1. Best Fit Parameters of DSC Data for Transferrin Binding of Ti(IV)

Ti(IV) equiv	T_m (°C)			ΔH_{N-U} (kcal/mol)		
	C		N	C		N
Apo	59.4		69.4	143.1		200.7
1	61.3[a,b]	66.2	70.3	87.9	126.0	200.9
	61.5[c]	63.3	71.2	123.0	68.7	205.1
2	65.0[a,b]	66.1	70.5	47.7	131.3	206.8
	64.0[c]	66.3	72.8	89.6	150.2	225.3

[a] The C lobe is fit to a two-domain model. [b] Data for titanocene dichloride. [c] Data for $Ti(citrate)_3^{8-}$.

Chart 2. N−Ti−N (θ) and O−Ti−O (ϕ) Angles of TiEHPG and TiHBED

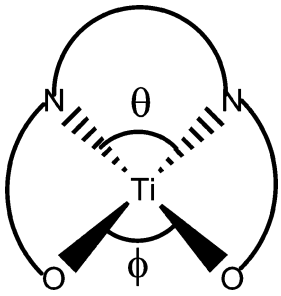

Water coordination in TiEHPG and its absence in TiHBED reflect the size of the central metal and the Ti−N bond lengths.[48] TiEHPG complexes have the longest M−N bonds of metal−EHPG complexes and the smallest N−M−N angles (θ = 72.44-(0.55)°) (Chart 2). Increasing the M−N bond lengths result in movement of the trans oxygen atoms and opening of the O−M−O angle (ϕ = 145.23(1.48)°) trans to the N−M−N angle, facilitating water coordination. In the TiHBED complex, the M−N bonds are slightly longer but the N−M−N angle (θ = 79.99(7)°) is bigger, comparable to the N−M−N angles of $FeEHPG^-$ and $FeHBED^-$.[80,81] The O−M−O angle (ϕ = 109.65(7)°) trans to N−M−N is also smaller than that in TiEHPG, and water coordination is precluded at low pH.

In aqueous solution a single TiHBED species exists from pH 3.0 to 4.0. Several TiHBED species appear to exist in the pH 7.0 to 9.0 range as suggested by ^{1}H NMR, UV−vis, and cyclic voltammetric studies. Mass spectrometry and NMR studies suggest that the structure of the pH 3.0 complex is the same as the crystallized structure.

The formation kinetics of TiHBED at pH 3.0 were investigated in a citrate substitution experiment. The observed rate constant for the monoexponentially fit data increased linearly with an increase in HBED concentration and decreased with an increase in citrate concentration. The evidence supports a dissociative mechanism in which $Ti(citrate)_3$ first dissociates to a $Ti(citrate)_2$ complex and then Ti(IV) is bound by HBED. From the temperature variation experiment, the activation energy of the second step was determined to be 64.4 kJ mol^{-1}. This value is comparable with the activation energy (55 kJ mol^{-1}) measured for the first phase of the reaction of Fe(III) pyro-

(80) Larsen, S. K.; Jenkins, B. G.; Memon, N. G.; Lauffer, R. B. *Inorg. Chem.* **1990**, *29*, 1147−1152.
(81) Bailey, N. A.; Cummins, D.; McKenzie, E. D.; Worthington, J. M. *Inorg. Chim. Acta* **1981**, *50*, 111−120.

phosphate with transferrin in the presence of bicarbonate.[82] The activation enthalpy measured was 61.7 kJ mol^{-1}. The activation entropy was -20.3 J mol^{-1} K^{-1}. The negative value suggests that the activated complex in the transition state has a more ordered structure than the reactants in the ground state. It is consistent with the formation of a ternary complex between HBED and Ti(citrate)$_2$ in the rate determining step.

The affinity of HBED^{4-} for Ti(IV) ($\log \beta = 34.074$) is about 5 orders of magnitude lower than that for Fe(III) (Table S6). This result is in contrast to the one found for transferrin binding.[26] The reversed stability trend may be due to HBED being a slightly softer ligand than transferrin. HBED, like EHPG, has one more nitrogen binding atom than transferrin and consequently one fewer charged oxygen binding atom.

Differences in attractive forces may also account for a lower stability of TiHBED. TiHBED is not readily soluble in water whereas FeHBED$^-$ is, most likely because the latter is anionic and can be stabilized by electrostatic attractions. FeHBED$^-$ is quite stable at pH 7.4 while TiHBED is susceptible to hydrolysis as indicated by the decrease in the LMCT absorbance at 370 nm and the shift of λ_{max} to a shorter wavelength. The binding of hydroxides and probably dissociation of some of the HBED binding atoms would be expected to change TiHBED into an anionic species.

It is interesting to note that transferrin can bind Ti(IV) in unhydrolyzed form at pH 7.4 whereas the model TiHBED is believed to exist as a hydrolyzed Ti(IV) species at this pH. Protein lobe closure following metal chelation by transferrin[24] results in the metal-binding sites of the C- and N-lobes being less solvent exposed. The metal coordination spheres are thus more protected from hydrolysis in the protein, and the metal−Tf complexes are stabilized by intramolecular hydrogen bonds and electrostatic attractions.

The reduction potential of TiHBED was also measured. A nearly reversible process ($E_{1/2} = -641$ mV vs NHE) was observed at pH 4.0. From these data, the stability constant of TiHBED$^-$ can be calculated:[83]

$$E_c - E_s = (-0.059/n)[\log(\beta_{IV}/\beta_{III})] \quad (5)$$

where β_{III} and β_{IV} are the Ti(III) and Ti(IV) HBED affinity constants,

$$Ti^{3+} + HBED^{4-} \overset{\beta_{III}}{\rightleftharpoons} TiHBED^- \quad (6)$$

$$Ti^{4+} + HBED^{4-} \overset{\beta_{IV}}{\rightleftharpoons} TiHBED \quad (7)$$

E_c and E_s are the potentials for the complex ion and the aqueous ion half-cells

$$TiHBED + e^- \rightleftharpoons TiHBED^- \qquad E_c = -641 \text{ mV} \quad (8)$$

$$Ti(OH)_2^{2+} + 2H^+ + e^- \rightleftharpoons Ti^{3+} + H_2O \qquad E_s = +0.099 \text{ V} \quad (9)$$

and n (=1) is the number of electrons involved in the redox process. β_{III} was calculated to be 4.6×10^{24}, suggesting that the affinity of HBED^{4-} for Ti(III) is 10 orders of magnitude weaker than its affinity for Ti(IV).

Transferrin Binding of Ti(IV). Fe(III) and other metals are generally bound by transferrin with a synergistic anion (usually carbonate) in a distorted octahedral geometry. With Ti(IV) there may be multiple modes of coordination (Figure 9) by transferrin, depending on pH, on the source of Ti(IV) used to load the protein, and on the availability of carbonate or another synergistic anion.

One mode could possibly be chelation as hydroxide- or oxide-bound Ti(IV). Bicarbonate is not needed to bind Ti(IV).[22] In recent work, EXAFS and preliminary crystallographic data indicated that Ti(IV) coordinates as a titanyl species to the ferric-ion binding protein from *Neisseria gonorrheae*.[49] The metal binding site of this protein is very similar to that of human serum transferrin. Other than direct coordination to the two tyrosines, the hydrated metal ion is bound to other residues via Ti−O bonds. The source of titanium in these studies[22,49] was titanocence dichloride, which is readily susceptible to hydrolysis and exists as an oxide species at pH 7.4.[78]

By avoiding metal ion hydrolysis, Ti(IV) can also coordinate to transferrin with bound synergistic anion. A ^{13}C NMR experiment using ^{13}C-enriched bicarbonate showed that carbonate is bound to Ti(IV) in transferrin. This evidence was previously shown.[22] In that work, performed with the hydrolysis-prone titanocene dichloride, the bound carbonate readily dissociated, possibly because of a weaker interaction with Ti(IV) through hydrogen bonding instead of direct coordination. The ^{13}C NMR signal due to coordinated bicarbonate was stable in the current study. Stopped-flow kinetic data showed that the rate of the initial phase of Ti$_2$−Tf formation increases with an increase in bicarbonate concentration even in the presence of excess citrate. However, in the absence of bicarbonate, transferrin does coordinate Ti(IV) but at a slower rate and with citrate believed to be serving as a synergistic anion. At pH values greater than 8.5 the carbonate or citrate may dissociate from Ti(IV) and be replaced by bound hydroxides or oxides. The extinction coefficient for the LMCT absorbance of this species is comparable to that reported for a Ti$_2$−Tf species prepared with titanocence dichloride and without bicarbonate.[22]

The different modes of Ti(IV) coordination impart a major difference in the holoprotein electronic spectrum. The molar absorptivity of the LMCT band measured at 321 nm for transferrin binding of 2 equiv of unhydrolyzed Ti(IV) is 20 760 M^{-1} cm^{-1}.[26] For 2 equiv of hydrolyzed Ti(IV) it is 4830 M^{-1} cm^{-1}.[22] Because this transition arises from a tyrosine to titanium charge transfer, the reduced value may reflect a lesser Tyr−Ti(IV) orbital−orbital overlap. The lesser overlap is proposed to be due to hydroxide coordination that may result in dissociation of some of the transferrin ligands as suggested in Figure 9. The molar absorptivity values are relative to protein concentration and are conditional; that is, they depend on the synergistic anion present, as is true for Fe(III) binding of transferrin.[22]

Transferrin coordination of Ti(IV) is modeled well by TiHBED. Below pH 3.0 and above pH 9.5, competition with protons and hydroxides, respectively, results in minimal coordination of Ti(IV) by either transferrin or HBED. TiHBED exhibits an LMCT molar absorptivity (9141 M^{-1} cm^{-1}) that compares favorably with that for Ti$_2$−Tf (10 380 M^{-1} cm^{-1}

(82) Cowart, R. E.; Swope, S.; Loh, T. T.; Chasteen, N. D.; Bates, G. W. *J. Biol. Chem.* **1986**, *261*, 4607−4614.
(83) Borgias, B. A.; Cooper, S. R.; Koh, Y. B.; Raymond, K. N. *Inorg. Chem.* **1984**, *23*, 1009−1016.

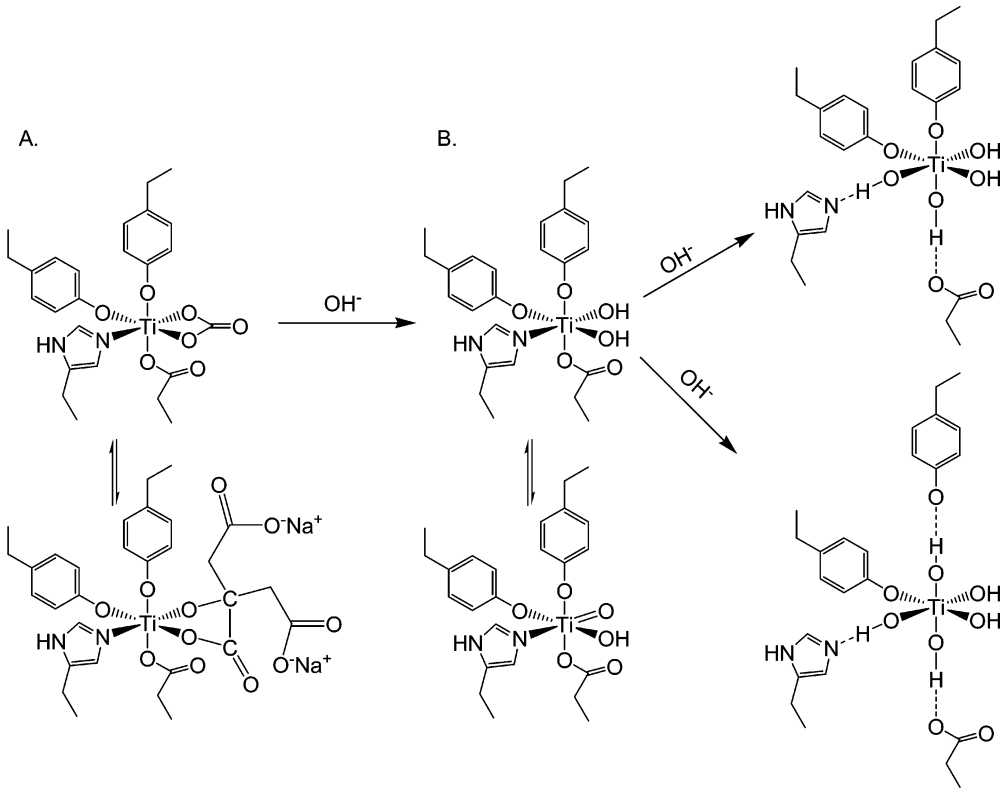

Figure 9. Proposed coordination of Ti(IV) by transferrin with bound synergistic anions (A) carbonate or citrate and with (B) Ti(IV)-bound hydroxide or oxide.

per lobe) although the absorbance is at a lower energy. When the metal ion becomes partially hydrolyzed at higher pH the LMCT molar absorptivity for TiHBED decreases by about 50%, similar to the decrease for Ti_2-Tf from pH 8.0 to 9.5. The fluorescence emission spectra of HBED and transferrin (λ_{ex} = 280 nm) are quenched to comparable extents when they bind Ti(IV). When HBED binds Ti(IV), deprotonation of the phenol rings results in perturbation of the $\pi-\pi^*$ transition. Transferrin binding of Ti(IV) results in deprotonation of the tyrosine residues, but the major contribution to quenching is the impact on the tryptophan residues due to global protein conformational changes.[84,85]

The study of the aqueous speciation of Ti_2−Tf and the comparisons drawn with that of TiHBED help to understand how transferrin may coordinate Ti(IV) in vivo.

Thermal Stability of Ti_2−Tf. Transferrin binding of Fe(III) as monitored by DSC involves lobe unfolding transition crossover.[79,86] In the apoprotein, the C-lobe unfolds at a lower temperature than the N-lobe. The temperature of the unfolding transition of the C-lobe becomes higher than that of the N-lobe after addition of 1 mol equiv of Fe(III). However, transferrin binding of Ti(IV) does not appear to involve significant C- and N-lobe interaction. Addition of Ti(IV) to transferrin via a partly hydrolyzed or unhydrolyzed source stabilized the C- and N-lobes, but only slightly as indicated by minor increases in the respective T_m values. The C-lobe with Ti(IV) bound undergoes a biphasic transition. Biphasic behavior is not very surprising considering that the two domains of the C- and N-lobes are not identical (Figure S15). This behavior was also observed for the thermal unfolding of the C-lobe of melanotransferrin,[87] which does not bind Fe(III). Transferrin lobes that are capable of binding metals more typically undergo monophasic transitions.[79] When the protein is fully saturated with Ti(IV), one of the transitions of the C-lobe dominates.

Given similar thermal stability results for the two forms of Ti_2−Tf, it appears that the different forms of Ti(IV) coordination by transferrin result in similar protein conformational changes. These changes do not stabilize transferrin with respect to temperature to the extent that Fe(III) does, as indicated by the higher monophasic transition T_m (87 °C) of Fe_2−Tf.[79] This result is surprising considering that Ti(IV) binds with greater affinity to transferrin at 25 °C[26] and Ti(IV) coordination quenches transferrin fluorescence emission (73%) about as much as Fe(III) does,[84] which could be correlated with comparable conformational changes and stability enhancement.

The thermal unfolding of the Ti_2−Tf complex is not reversible, which is also true of the Fe_2−Tf complex.[79] Therefore, binding constants derived from the DSC data would be misleading. In the current work, the irreversibility of the DSC experiment underscores the fact that Ti_2−Tf binding is not under thermodynamic control. Although the formal binding for putative aquated Ti(IV) is quite tight, the thermodynamic sink overall favors titanium hydrolysis and precipitation as TiO_2. The Ti_2−Tf complex is thus best described as metastable, and the elevated temperature of the DSC experiment promotes irreversible metal release. It should be noted that the temperature at which this release occurs is well above physiological temperature.

(84) Lehrer, S. S. *J. Biol. Chem.* **1969**, *244*, 3613−3617.
(85) He, Q.-Y.; Mason, A. B.; Lyons, B. A.; Tam, B. M.; Nguyen, V.; MacGillivray, R. T. A.; Woodworth, R. C. *Biochem. J.* **2001**, *354*, 423−429.
(86) Brandts, J. F.; Hu, C. Q.; Lin, L. N. *Biochemistry* **1989**, *28*, 8588−8596.
(87) Creagh, A. L.; Tiong, J. W. C.; Tian, M. M.; Haynes, C. A.; Jefferies, W. A. *J. Biol. Chem.* **2005**, *280*, 15735−15741.

Relevance to Ti(IV) Transport. Fe(III) is transported into cells via the transferrin receptor-mediated endocytosis pathway following complexation by transferrin.[24,88] It is postulated that Fe(III) is released from transferrin in the endosomes partly by reduction to Fe(II). The reduction potential of Fe(III)-loaded transferrin is ~ -500 mV, which is too low to be reduced by physiological reductants at endosomal pH (5.8).[89,90] However, the transferrin receptor raises the reduction potential by more than 200 mV.[91] The free Fe(II) is then transported to the divalent metal transporter 1 (DMT1) and released into the cell.[92] The electrochemistry of metal complexes of EHPG and HBED appears to model well the electrochemistry of metal-loaded transferrin. The $E_{1/2}$ for $FeEHPG^-$ at pH 6.0 is -480 mV,[93] similar to that for Fe_2-Tf. The magnitude of the TiHBED reduction potential ($E_{1/2} = -641$ mV) suggests that the reduction potential of Ti(IV)-loaded transferrin would be even lower than that of Fe(III)-loaded transferrin. Even if the transferrin receptor could raise the reduction potential of Ti(IV) to a physiologically reducible level, further reduction of the metal to Ti(II) would probably not be possible. Questions thus arise about how the metal would be transported out of the endosomes, especially if DMT1 is really specific for soft/intermediate divalent metal ions.[92] Certainly, reduction of Ti(IV) would weaken the affinity of transferrin for the metal as it does for HBED, but it is uncertain whether this mode of metal release from transferrin is superior to direct chelation of the oxidized metal ion by a cellular ligand such as ATP, as has been proposed.[22]

Conclusion

The work conducted in this study has addressed some of the questions regarding transferrin binding of Ti(IV). Work with $Ti(citrate)_3$, a highly stable form of Ti(IV) when excess citrate is present, and titanocene dichloride, a hydrolysis-prone species, has revealed that transferrin can coordinate Ti(IV) with and without hydroxide (or oxide). pH stability studies reveal that Ti(IV) saturation of transferrin is highly pH dependent and that the synergistic anions, carbonate and citrate, can easily be displaced by hydroxide at pH values greater than 8.5. Thermal stability studies suggest that Ti_2-Tf is a metastable complex with Ti(IV) thermodynamically drawn to irreversible dissociation as TiO_2. These findings help to understand the factors that affect the integrity of Ti_2-Tf and the possible transport of Ti(IV) by transferrin in cells.

Crystallographic and extensive solution dynamic studies are warranted with the native protein to determine the physiologically relevant chelation of Ti(IV). This investigation would help direct Ti(IV) drug development, especially if the transport of Ti(IV) as a titanyl unit into cells is essential for anticancer activity.[94,95]

Acknowledgment. We are grateful to Ritika Uppal, Cynthia Peterson, and Suzanna Milheiro for their assistance. We also thank Dr. Nigel Grindley for use of his fluorimeter, Dr. Donald Crothers for use of his Cary 100, Dr. Helmut Ernstberger for his help with cyclic voltammetry, Dr. Jeff Hoch and Zandra Sutter for their help with differential scanning calorimetry, and the Keck Foundation Biotechnology Research Laboratory at Yale University for use of the dynamic light scattering instrument. We thank the Thomas Shortman Training, Scholarship, and Safety Fund for a fellowship (A.D.T.) and the American Cancer Society New England Division Research Scholar Grant for funding this work. A special thanks is given to the support of Ana M. Tinoco and Angel A. Tinoco, without which this work would never have been possible.

Supporting Information Available: X-ray crystallographic data for TiHBED (PDF, CIF). ^1H and proton-decoupled ^{13}C NMR data and fluorescence emission data for TiHBED and Ti_2-Tf. Electrospray mass spectrometric data for TiHBED and Ti(citrate). Arrhenius and Eyring plots corresponding to the variable temperature kinetic experiments of the formation of TiHBED. Speciation data and binding equations for TiHBED. Thermal spectrophotometric denaturation data for Ti_2Tf. This material is available free of charge via the Internet at http://pubs.acs.org.

JA068149J

(88) Qian, Z. M.; Li, H.; Sun, H.; Ho, K. *Pharm. Rev.* **2002**, *54*, 561−587.
(89) Kretchmar, S. A.; Reyes, Z. E.; Raymond, K. N. *Biochim. Biophys. Acta* **1988**, *956*, 85−94.
(90) Kraiter, D. C.; Zak, O.; Aisen, P.; Crumbliss, A. L. *Inorg. Chem.* **1998**, *37*, 964−968.
(91) Dhungana, S.; Taboy, C. H.; Zak, O.; Larvie, M.; Crumbliss, A. L.; Aisen, P. *Biochemistry* **2004**, *43*, 205−209.
(92) Garrick, M. D.; Dolan, K. G.; Horbinski, C.; Ghio, A. J.; Higgins, D.; Porubcin, M.; Moore, E. G.; Hainsworth, L. N.; Umbreit, J. N.; Conrad, M. E.; Feng, L.; Lis, A.; Roth, J. A.; Singleton, S.; Garrick, L. M. *Biometals* **2003**, *16*, 41−54.
(93) Gómez-Gallego, M.; Pellico, D.; Ramirez-López, P.; Mancheño, M. J.; Romano, S.; de la Torre, M. C.; Sierra, M. A. *Chem.—Eur. J.* **2005**, *11*, 5997−6005.
(94) Duffy, B.; Schwietert, C.; France, A.; Mann, N.; Culbertson, K.; Harmon, B.; McCue, J. P. *Biol. Trace Element Res.* **1998**, *64*, 197−213.
(95) Schwietert, C. W.; Yaghoubi, S.; Gerber, N. C.; McSharry, J. J.; McCue, J. P. *Biol. Trace Element Res.* **2001**, *83*, 149−167.